Drugs of the Future 2005, 30(3): 254-260

CCC: 0377-8282/2005
DOI: 10.1358/dof.2005.030.03.886482

Taltobulin

Prop INN

Oncolytic Drug
Tubulin Polymerization Inhibitor
Antimitotic Drug

HTI-286
SPA-110

N,3,3-Trimethyl-L-phenylalanyl-N^1-[3-carboxy-1(*S*)-isopropyl-2(*E*)-butenyl]-N^1,3-dimethyl-L-valinamide

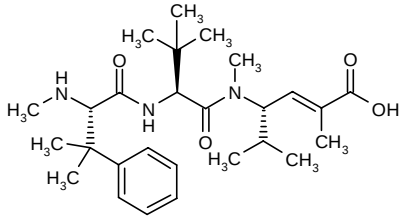

$C_{27}H_{43}N_3O_4$

Mol wt: 473.6537

CAS: 228266-40-8

EN: 317936

Abstract

Antimicrotubule agents are among the most effective drugs for the treatment of breast, ovarian and other forms of cancer. Two classes of antimicrotubule drugs are commonly used: the taxanes, which accelerate tubulin polymerization by stabilizing assembled microtubules and obstructing depolymerization, and the *Vinca* alkaloids, which bind to the tubulin α/β-heterodimer, block the formation of normal microtubules and lead to the depolymerization of microtubules and/or the formation of abnormal tubulin polymers. While these drugs inhibit tumor progression, their cytotoxic effects on rapidly proliferating normal tissues and other significant side effects are limiting factors. In addition, inherent resistance to antimicrotubule agents is encountered in many tumor types, or acquired resistance may occur during multiple cycles of therapy. Thus, there is great interest in and an unmet need for identifying novel antimicrotubule drugs. Taltobulin (HTI-286, SPA-110) is a novel antimitotic agent that inhibits the polymerization of tubulin, disrupts microtubule dynamics in cells and induces mitotic arrest and apoptosis. Relative to the antimicrotubule drugs in use, taltobulin exhibits significantly less interaction with the multidrug resistance protein (P-glycoprotein) and is effective in inhibiting human tumor xenografts in nude mouse models where paclitaxel and vincristine are ineffective. Taltobulin administered i.v. or p.o. in saline inhibits the growth of numerous human tumors without the side effects associated with formulations. Taltobulin is in clinical development.

Synthesis

The synthesis of taltobulin is achieved through a convergent route depicted in Schemes 1-3. Individual building blocks (VI), (XV) and (XIV) are prepared and the final skeleton put together by sequential peptide coupling of the units. The *E*-double bond configuration in (XIV) is established through a Wittig olefination reaction. The desired *S*,*S*,*S* stereochemistry is achieved using chiral synthons for the construction of the (XVII) portion and a stereoselective synthesis of (VI), or alternatively, racemic synthesis of (X) and resolution to get (VI), or the use of racemic (X) and separation of the resulting *R*,*S*,*S*- and *S*,*S*,*S*-diastereomers.

The stereoselective synthesis of (VI) (1) is shown in Scheme 1. The synthesis of 3-methyl-3-phenylbutanoic acid (II) is accomplished by heating 3,3-dimethylacrylic acid (I) and aluminum chloride in benzene. For stereoselective introduction of the α-amino group, Evans' chiral auxiliary method is used. Reaction of (II) with pivaloyl chloride gives the corresponding mixed anhydride, which upon treatment with the lithiated oxazolidinone provides amide (III). Treatment of (III) with base followed by triisopropylphenylsulfonyl azide gives the corresponding azide (IV). Reduction of (IV) to the amine in the presence of di-*tert*-butyl dicarbonate followed by lithium hydroperoxide-promoted removal of the chiral auxiliary provides the phenylalanine derivative (V). Introduction of the *N*-methyl group is accomplished by treatment of (V) with NaH and MeI in DMF, followed by hydrolysis of the resulting methyl ester to provide the Boc-protected trimethylphenylalanine derivative, the desired building block (VI) bearing the *S*-configuration (1, 2).

A shorter synthesis of racemic (VI), (X), starts with the readily available phenylpyruvic acid (VII) (1, 2). Dimethylation of the latter using base and methyl iodide yields (VIII). Reductive amination of (VIII) using methylamine gives the racemic phenylalanine derivative (IX).

S. Ayral-Kaloustian, A. Zask. Wyeth Research, Pearl River, NY 10965, USA.

Scheme 1: Synthesis of Intermediate VI

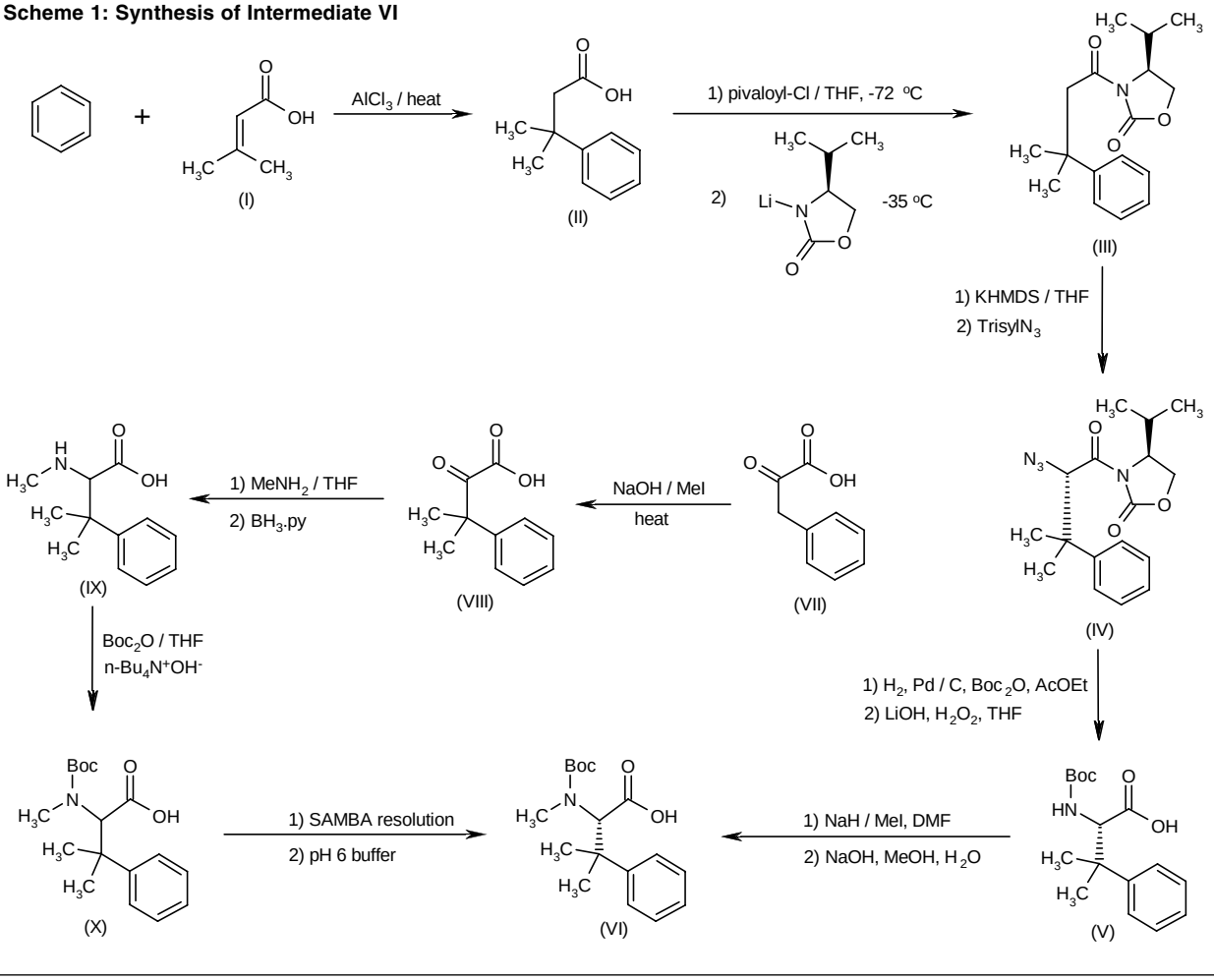

Scheme 2: Synthesis of Intermediate XVII

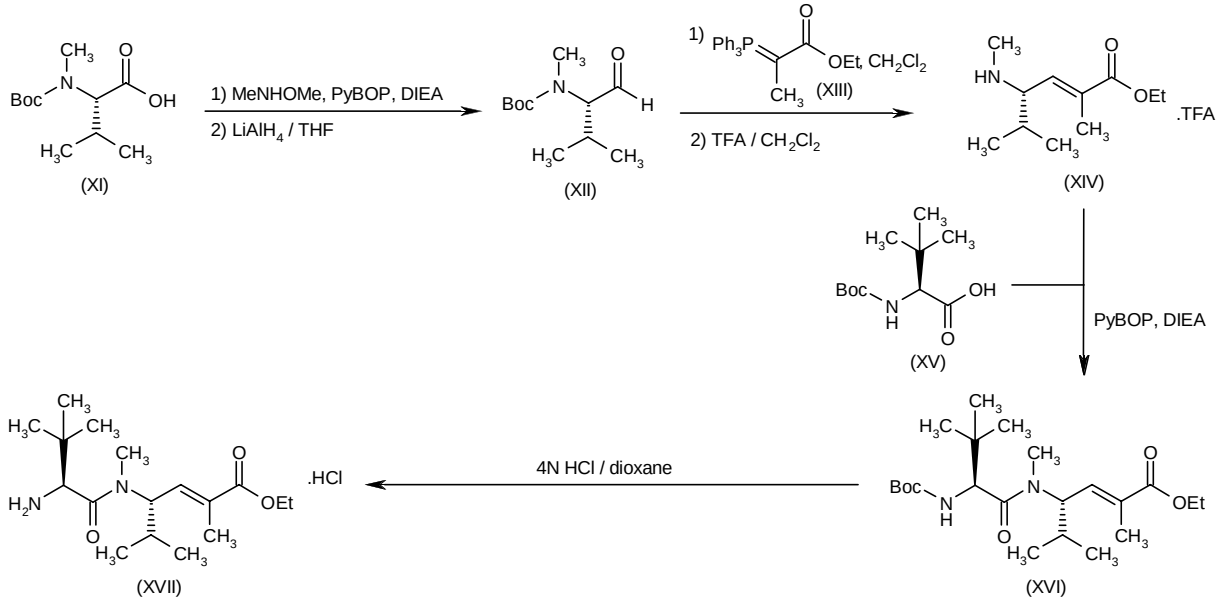

Scheme 3: Synthesis of Taltobulin

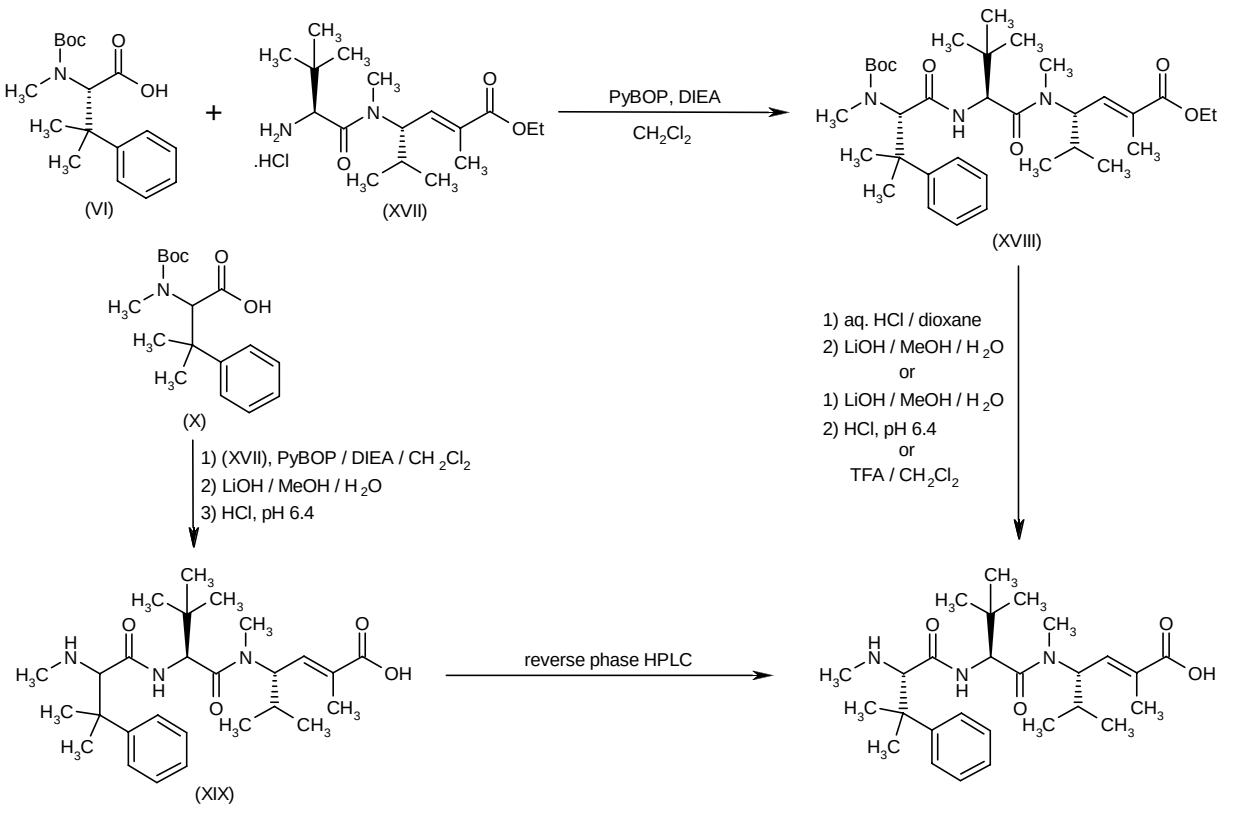

Protection of (IX) with di-*tert*-butyl dicarbonate provides racemic (X).

Building block (XVII) is synthesized from commercially available *N*-Boc-protected L-amino acids (XI) and (XV) as shown in Scheme 2 (1-3). Compound (XI) (*N*-Boc-*N*-methyl-L-valine) is converted to the corresponding valinal (XII) via formation of the Weinreb amide, and reduction of the latter with $LiAlH_4$ in tetrahydrofuran. The reaction of (XII) with the stabilized Wittig reagent (XIII) ([1-(ethoxycarbonyl)ethylidene]triphenylphosphorane) in CH_2Cl_2, followed by removal of the *N*-Boc group with TFA in CH_2Cl_2, provides, stereoselectively, the desired *E*-2-alkenoate (XIV) as the TFA salt. The latter is coupled with the commercially available amino acid (XV) (*N*-Boc-L-*tert*-Leu), using PyBOP and excess *N,N*-diisopropylethylamine to give intermediate (XVI). Removal of the Boc group with hydrochloric acid in dioxane provides the desired building block (XVII) as the HCl salt.

Formation of the taltobulin scaffold is achieved by coupling the building block (VI) with (XVII), using PyBOP in CH_2Cl_2, as shown in Scheme 3 (1). The resulting protected intermediate (XVIII) is converted to taltobulin via sequential removal of the ethyl ester and Boc groups under standard conditions, in either order. Thus, hydrolysis of the *N*-Boc group under acidic conditions, followed by saponification of the ethyl ester, gives taltobulin (1, 2), and reversing the order provides either taltobulin (using buffered acid) or one of its salts (*e.g.*, TFA or HCl), as desired (1-3). On a small scale, the product is purified by reverse-phase HPLC to provide the TFA salt. In bulk quantities, pure taltobulin is isolated by trituration or crystallization (1).

A shorter path to taltobulin makes use of the readily available racemic (VI), (X) (Scheme 1). Reaction of the latter with (XVII) under standard coupling conditions and deprotection gives (XIX) as a mixture of the *R*,*S*,*S*- and *S*,*S*,*S*-diastereomers. Alternatively, the unprotected intermediate (IX) (Scheme 1) is coupled with (XVII) and the resulting ester hydrolyzed to yield (XIX). Reverse-phase HPLC of (XIX) yields pure taltobulin as the TFA salt (1, 2).

Introduction

Microtubules are large, dynamic cellular structures with many functions, including the formation of the mitotic spindle and chromosomal separation (mitosis), control of cell shape and motility, and intracellular transport and signaling. Antimicrotubule agents promote cell death (apoptosis) by interfering with tubulin-microtubule dynamics, and with the formation and function of the mitotic spindle, thereby preventing chromosomal separation and

inducing mitotic arrest (4-7). Chemically diverse tubulin-binding agents, most of which are natural products or derived from natural products, target a variety of tubulin binding sites and have been shown to inhibit microtubule function and tumor growth *in vitro* and *in vivo* in xenograft models (1, 3, 6-9). When used in stoichiometric concentrations, these agents work mainly as cytotoxic agents, by either increasing or decreasing the cellular microtubule mass. Thus, the two classes of antimitotic drugs commonly used in the clinic for the treatment of breast, ovarian and other forms of cancer have different sites and modes of binding to tubulin and differ in their mechanism of action. The taxanes (*e.g.*, paclitaxel and docetaxel) stabilize microtubules against depolymerization, and the *Vinca* alkaloids (*e.g.*, vinorelbine, vinblastine and vincristine) bind to the tubulin dimer, block the formation of new microtubules and lead to the depolymerization of existing microtubules. It has been shown that at lower concentrations both groups of drugs can lead to mitotic arrest and apoptosis, without affecting the cellular microtubule mass. Hence, the observed inhibition of tumor growth can be attributed to a combination of these cytotoxic and apoptotic effects. While these drugs have been effective in inhibiting the progression of certain types of tumors, their cytotoxic effects on rapidly proliferating normal tissues (*e.g.*, gastrointestinal tract, hair follicles, bone marrow), and other significant side effects resulting from either the compounds themselves and/or the vehicle required for administration, are limiting factors. In addition, inherent resistance to antimicrotubule agents is encountered in many tumor types, or acquired resistance may occur during multiple cycles of therapy (4, 10). Therefore, many patients are treated with these toxic agents without receiving an anticancer benefit. Thus, there is great interest in, and an unmet need for, the development of novel antimicrotubule drugs that can overcome the various forms of resistance and exhibit improved pharmacokinetic properties.

Antimicrotubule drugs under clinical investigation include novel taxanes, the epothilones, the combretastatins, discodermolide, the halicondrins, cryptophycin-52 and other peptide-like agents (*e.g.*, dolastatin-10, cemadotin and the hemiasterlin analogue taltobulin) (1, 6, 11, 12). Hemiasterlins isolated from marine sponges (*Hemiasterella minor*, *Cymbastella* spp., *Auletta* spp. and *Siphonochalina* spp.) consist of a small family of naturally occurring tripeptides (13-15) with potent effects on tubulin which make them especially attractive as drugs. Hemiasterlin is a potent inhibitor of cell growth and induces cell cycle arrest at the G_2-M phase (16). This effect is due to the induction of the formation of ring-like tubulin aggregates, and like the *Vinca* alkaloids, depolymerizing or destabilizing microtubules (17). Furthermore, as observed with other peptide-like antimicrotubule agents, hemiasterlin is a noncompetitive inhibitor of the binding of vinblastine to tubulin. In contrast, hemiasterlin competitively inhibits the binding of dolastatin-10 to tubulin. Therefore, it has been proposed that this class of small peptides binds to the β-tubulin unit of the α/β-heterodimer at a binding site ("peptide site") that is close to but distinct from the *Vinca* binding site (8, 17). Synthetic methods for producing hemiasterlin and its analogues (1-3, 18) have allowed the evaluation of many related compounds and a better understanding of the binding of these peptide-like molecules with tubulin (19, 20).

Taltobulin (HTI-286, SPA-110), a synthetic analogue of hemiasterlin wherein a phenyl group replaces the indole ring, is a novel antimitotic agent. As observed with hemiasterlin itself, taltobulin inhibits the polymerization of purified tubulin, disrupts microtubule organization in cells, and induces mitotic arrest and apoptosis (11). It is a very potent inhibitor of proliferation, with a mean IC_{50} of 2.5 nM against 18 human tumor cell lines. Taltobulin is a poor substrate for P-glycoprotein (P-gp) and, relative to currently used antimicrotubule agents, is considerably more effective in preventing the growth of resistant tumors that express P-gp. Therefore, the compound is effective in inhibiting the growth of human tumor xenografts in nude mouse models where paclitaxel and vincristine are found to be ineffective (11). Taltobulin is composed of highly unusual and sterically congested amino acids which confer stability to the molecule, as with the natural hemiasterlins, thus providing good bioavailability and *in vivo* activity. Taltobulin administered i.v. or p.o. as a solution in saline circumvents the side effects that can result from the use of a vehicle, and effectively inhibits the growth of numerous human tumor xenografts (skin, breast, prostate, brain and colon cancers). Marked tumor regression is observed in nude mice when the compound is used to treat established tumors that are > 1 g in size (11). Therefore, taltobulin was selected for further development for the treatment of advanced malignant solid tumors.

Pharmacological Actions

Based on analogy with competitive binding studies done with hemiasterlin (8, 17), taltobulin is proposed to bind at the peptide site, close to the *Vinca* binding site on tubulin. Hemiasterlin and other antimitotic peptides (dolastatin-10, phomopsin A and cryptophycin 1) noncompetitively inhibit the binding of vinblastine to tubulin, but competitively inhibit each other's binding to tubulin. Two radiolabeled benzophenone analogues of taltobulin, used as photoaffinity probes for the tubulin-binding site, were found to crosslink exclusively to amino acid residues in α-tubulin proximal to the *Vinca* binding site. The peptide sequences have longitudinal interactions with β-tubulin across the interdimer interface (19).

Taltobulin was found to oligomerize tubulin to a discrete ring structure consisting of about 13 tubulin units, as determined by sedimentation equilibrium analysis (21). The use of a stilbene analogue of taltobulin with a unique chromophore, distinct from protein, indicated that the binding stoichiometry in this ring is 1 inhibitor per tubulin unit (20).

A comprehensive investigation of the effects of taltobulin *in vitro* and *in vivo* has been conducted (11). These studies focused on the efficacy of taltobulin in tumor cells expressing P-gp, which are resistant to anticancer agents such as paclitaxel. The effect of taltobulin on tubulin and its cytotoxicity in tumor cells were explored. Thus, in a cell-free system taltobulin at a concentration of 0.1 μM inhibited the polymerization of purified bovine tubulin by 41%. This effect was comparable to that of vincristine (30%) at the same concentration. In contrast, at 1 μM taltobulin and vincristine totally inhibited polymerization, whereas colchicine showed only partial inhibition. Taltobulin was also able to permeate cells and interfere with microtubule polymerization. In KB-3-1 epidermoid carcinoma cells, taltobulin disrupted the appearance of microtubules in a concentration-dependent manner. After 3 days of treatment with 1 nM of taltobulin (the IC_{50} for inhibition of cell growth), cells were rounded and 50% were arrested in metaphase. At higher concentrations (16 nM), few microtubules were seen and the cells showed diffuse cytoplasmic staining. As with other antimicrotubule agents, taltobulin induced a concentration-dependent increase in cells arrested at mitosis (G_2-M). Thus, at 10 nM, taltobulin arrested 90% of KB-3-1 cells at mitosis after 24 h. After 2-3 days of exposure, cells underwent concentration-dependent apoptosis.

Taltobulin was also shown to be a potent inhibitor of tumor cell growth (11) using 18 human tumor cell lines, being more potent than the clinically used anticancer agent paclitaxel (mean IC_{50} = 2.5 nM *vs.* 128 nM). In addition, taltobulin retained its effect in cells that overexpress P-gp. Whereas paclitaxel was 20-fold less effective in cells that expressed moderate to high levels of P-gp compared with cells that did not express P-gp, taltobulin was only 3.5-fold less active. Furthermore, KB-8-5 cells that express moderate levels of P-gp were moderately resistant (7-52-fold) to paclitaxel, docetaxel, vinblastine, vinorelbine, colchicine, dolastatin-10 and doxorubicin, but sensitive to taltobulin (only 2.4-fold resistance). KB-V1 cells expressing very high levels of P-gp were extremely resistant (1,400-1,800-fold) to paclitaxel, vinorelbine and vinblastine, but much more sensitive to taltobulin (only 81-fold resistance). No resistance to taltobulin was seen in cells overexpressing the drug transporters MRP1 and MXR (*e.g.*, HL-60 and S1 cells, respectively).

Taltobulin was effective in prestaged tumor xenograft models in athymic mice (11). At the maximum tolerated i.v. dose (MTD) of 1.6 mg/kg (days 1, 5 and 9), taltobulin inhibited tumor growth by approximately 96% on day 12 in mice bearing small established (100 mg) paclitaxel-sensitive Lox melanoma or KB-3-1 epidermoid carcinoma. The minimum effective dose (MED) of taltobulin in the Lox melanoma model was about 0.2 mg/kg. Thus, the therapeutic index (MTD/MED), a measure of tolerability, was about 8. Taltobulin was also effective against other paclitaxel-sensitive tumor xenografts (PC-3-MM2 prostate carcinoma, SW620 colon carcinoma, U-87 MG glioma, MCF7 breast carcinoma and LoVo colon carcinoma). Taltobulin (1.6 mg/kg i.v. on days 1, 5 and 9) inhibited growth by 84% on day 14 (growth resumed by day 21) in xenograft models using tumors derived from P-gp-expressing, paclitaxel-resistant KB-8-5 cells. These tumors were not responsive to standard doses of 60 mg/kg of paclitaxel or 1 mg/kg of vincristine. Similarly, tumors derived from MX-1W human breast carcinoma cells inherently resistant to paclitaxel or vincristine showed 97% tumor growth inhibition when treated with taltobulin (1.6 mg/kg i.v. on days 1, 5 and 9), with an MED of about 0.7 mg/kg. Furthermore, complete inhibition of tumor growth could be maintained for greater than 8 weeks upon weekly administration of taltobulin. Taltobulin was also effective in xenograft studies using tumors derived from DLD-1 and HCT-15 human colon carcinoma cells with inherent paclitaxel resistance. In general, higher doses of taltobulin were required to treat mice bearing paclitaxel-resistant tumors compared to animals bearing paclitaxel-sensitive tumors. However, the higher doses of taltobulin required in these studies with resistant tumors were still well tolerated. Taltobulin was also effective in xenograft models of large established tumors (Lox melanoma, KB-3-1, LoVo and PC-3-MM2). For example, treatment of mice bearing Lox melanoma tumors (2.5 g) with taltobulin (1.6 mg/kg i.v.) weekly for 4 cycles resulted in inhibition of growth within 4 days of the first dose and eventually led to a 93% reduction in tumor size. Efficacy was also seen with intermittent dosing with multiple cycles of 1-3 weeks. Taltobulin was also effective after oral administration. In studies with Lox melanoma xenografts in athymic mice, oral dosing of taltobulin (3 mg/kg on days 1, 5 and 9) inhibited tumor growth by 97% on day 14. Oral efficacy for taltobulin (3 mg/kg) was also seen on day 22 upon weekly dosing in animals bearing KB-3-1 epidermoid xenografts. Oral activity for taltobulin indicates that it overcomes MDR1 expressed by gastrointestinal epithelial cells which limits the absorption of drugs such as paclitaxel that are substrates for MDR1.

In a study to determine potential mechanisms of resistance induced by exposure to taltobulin, KB-3-1 epidermoid carcinoma cells were exposed to increasing concentrations of drug for a period of nearly 1 year (22). Cells exposed to 2.5 and 4.0 nM of taltobulin were isolated. These cell lines, termed KB-2.5-HTI and KB-4.0-HTI cells, respectively, were 9-14-fold resistant to taltobulin and were also resistant to other compounds that bind to the *Vinca* peptide site on tubulin, such as dolastatin-10 (18-28-fold) and phomopsin A (5-fold). Crossresistance (5-14-fold) was also found for vinblastine and vinorelbine, which bind in the *Vinca* domain of tubulin. Agents such as colchicine, paclitaxel and epothilone B, which bind to sites distinct from these agents, showed minimal resistance in these cells. Similarly, in *in vivo* studies, tumors derived from KB-2.5-HTI cells in athymic mice failed to respond to taltobulin but did respond to paclitaxel. The KB-2.5-HTI and KB-4.0-HTI cells did not overexpress P-gp, BCRP, MRP1 or MRP3. The KB-4.0-HTI cells had a point mutation in α-tubulin that substitutes Ser for Ala12 near the nonexchangeable GTP-binding site. In a separate study, 1A9 ovarian carcinoma cells were subjected to

chronic taltobulin exposure. The resulting taltobulin-resistant cells, named 1A9-HTI-R, displayed enhanced sensitivity to taxanes and other tubulin-polymerizing drugs, were crossresistant to *Vinca* alkaloids and other hemiasterlins, lacked MDR1 and contained mutations in either α- or β-tubulin (23).

Pharmacokinetics and Metabolism

In vitro metabolism studies with taltobulin (50 μM) incubated for 2 h in liver microsomes from 4 different species (nude mice, rats, dogs and humans) revealed similar profiles (24). The predominant metabolite (M1) found in all 4 species was the pharmacologically inactive compound which is *N*-demethylated at the N-terminus. Rats and dogs received [^{14}C]-taltobulin (224 and 18.2 μg/kg i.v., respectively) and plasma, feces and urine samples were collected. Taltobulin was the major component in plasma and M1 was the only metabolite observed. Fecal excretion was the major elimination pathway for taltobulin and many metabolites were seen, including M1. Renal excretion was a minor elimination route (15%) for several metabolites observed, but among these only taltobulin and M1 were identified.

In vivo pharmacokinetic/metabolism studies were conducted in female nude and CD-1 mice, and in rats and dogs. Animals were given a single i.v. dose of taltobulin and plasma samples were collected over 24 h and analyzed for drug (25). Taltobulin showed a biphasic elimination profile and dose-proportional pharmacokinetics in all species. A high clearance and high volume of distribution over a broad range of doses were seen in all species. Using allometric scaling, these data were used to predict human pharmacokinetic parameters, and for dose selection in support of clinical studies. The predicted CL_T, Vd_{ss} and $t_{1/2}$ values for a 70-kg person were 0.544 l·h/kg, 6.93 l/kg and 8.8 h, respectively. These values were found to be reasonable approximations of those obtained in the clinic (CL_T, Vd_{ss} and $t_{1/2}$ for a 77.6-kg subject were 0.267 l·h/kg, 2.00 l/kg and 8.4 h, respectively). Based on these predictions and other pharmacological data, the effective dose in a 70-kg subject was estimated to be about 0.64 mg.

Clinical Studies

An open-label phase I study was conducted in 25 patients with metastatic or advanced malignant solid tumors, including gastrointestinal, renal, sarcoma, lung and other cancers, to assess the safety, tolerability and pharmacokinetics of taltobulin (26). Taltobulin was administered over 30 min as an i.v. solution in saline once every 3 weeks at doses ranging from 0.06 to 2.0 mg/m^2. The median age of the patients (18 males and 8 females) was 60 years. Common toxicities included neutropenia, nausea/emesis, alopecia and pain. Two patients exhibited grade 4 neutropenia (at 0.48 and 2 mg/m^2). Dose-limiting toxicities were grade 3 pain, grade 3 hypertension and grade 4 neutropenia. Preliminary pharmacokinetic data revealed considerable interindividual variability in clearance (15.7 ± 9.3 l/h), Vd_{ss} (177 ± 68 l) and half-life (9.2 ± 3.8 h). These were independent of dose and body surface area. Although neutropenia (ANC nadir) was associated with dose (r = –0.39) and AUC (r = –0.57), it was better correlated with time above 0.5 ng/ml (r = –0.64, p = 0.0004). A similar correlation could be obtained with the terminal elimination rate constant (l) normalized for dose (dose/l, r = –0.64). The phase II dose of taltobulin derived from this study appeared to be 1.5 mg/m^2 (or 3 mg) (26).

Sources

Wyeth Research (US); licensed from the University of British Columbia (CA).

References

1. Nieman, J.A., Coleman, J.E., Wallace, D.J., Piers, E., Lim, L.Y., Roberge, M., Andersen, R.J. *Synthesis and antimitotic/cytotoxic activity of hemiasterlin analogues.* J Nat Prod 2003, 66: 183-99.

2. Wu, Y., Megati, S., Gletsos, C., Kendall, J.T., Wilk, B.K., Padmanathan, T., Raveendranath, P. (Wyeth). *Process for the synthesis of intermediates useful for the synthesis of tubulin inhibitors.* US 2004063904, WO 0426814.

3. Zask, A., Birnberg, G., Cheung, K., Kaplan, J., Niu, C., Norton, E., Suayan, R., Yamashita, A., Cole, D., Tang, Z. et al. *Synthesis and biological activity of analogues of the antimicrotubule agent N,β,β-trimethyl-L-phenylalanyl-N^1-[(1S,2E)-3-carboxy-1-isopropylbut-2-enyl]-N1,3-dimethyl-L-valinamide (HTI-286).* J Med Chem 2004, 47: 4774-86.

4. Rowinsky, E.K., Tolcher, A.W. *Antimicrotubule agents.* In: Cancer Principles and Practice, Vol. 6. V.T. Devita Jr., S. Hellman, S.A. Rosenberger (Eds.), Lippincott Williams and Wilkins, Philadelphia, 2001, 431-52.

5. Jordan, M.A., Wilson, L. *Microtubules and actin filaments: Dynamic targets for cancer chemotherapy.* Curr Opin Cell Biol 1998, 10: 123-30.

6. Jordan, M.A., Wilson, L. *Microtubules as a target for anticancer drugs.* Nat Rev Cancer 2004, 4: 253-65.

7. Beckers, T., Mahboobi, S. *Natural, semisynthetic and synthetic microtubule inhibitors for cancer therapy.* Drugs Fut 2003, 28: 767-85.

8. Hamel, E., Covell, D.G. *Antimitotic peptides and depsipeptides.* Curr Med Chem - Anti-Cancer Agents 2002, 2: 19-53.

9. Ireland, C.M., Aalbersberg, W., Andersen, R.J., Ayral-Kaloustian, S., Berlinck, R.G.S., Bernan, V., Carter, G. et al. *Anticancer agents from unique natural products.* Pharm Biol 2003, 41(Suppl. 1): 15-38.

10. Gottesman, M.M. *Mechanisms of cancer drug resistance.* Annu Rev Med 2002, 53: 615-27.

11. Loganzo, F., Discafani, C.M., Annable, T. et al. *HTI-286, a synthetic analogue of the tripeptide hemiasterlin, is a potent*

antimicrotubule agent that circumvents P-glycoprotein-mediated resistance in vitro and in vivo. Cancer Res 2003, 63: 1838-45.

12. Kavallaris, M., Verrills, N.M., Hill, B.T. *Anticancer therapy with novel tubulin-interacting drugs.* Drug Resist Updates 2001, 4: 392-401.

13. Coleman, J.E., de Silva, E.D., Kong, F., Andersen, R.J., Allen, T.M. *Cytotoxic peptides from the marine sponge Cymbastela sp.* Tetrahedron 1995, 51: 10653-62.

14. Talpir, R., Benayahu, Y., Kashman, Y., Pannell, L., Schleyer, M. *Hemiasterlin and geodiamolide TA; two new cytotoxic peptides from the marine sponge Hemiasterella minor (Kirkpatrick).* Tetrahedron Lett 1994, 35: 4453-6.

15. Gamble, W.R., Durso, N.A., Fuller, R.W., Westergaard, C.K., Johnson, T.R., Sackett, D.L., Hamel, E., Cardellina, J.H. II, Boyd, M.R. *Cytotoxic and tubulin-interactive hemiasterlins from Auletta sp. and Siphonochalina spp. sponges.* Bioorg Med Chem 1999, 7: 1611-5.

16. Anderson, H.J., Coleman, J.E., Andersen, R.J., Roberge, M. *Cytotoxic peptides hemiasterlin, hemiasterlin A and hemiasterlin B induce mitotic arrest and abnormal spindle formation.* Cancer Chemother Pharmacol 1997, 39: 223-6.

17. Bai, R., Durso, N.A., Sackett, D.L., Hamel, E. *Interactions of the sponge-derived antimitotic tripeptide hemiasterlin with tubulin: Comparison with dolastatin 10 and cryptophycin 1.* Biochemistry 1999, 38: 14302-10.

18. Andersen, R.J., Coleman, J.E., Piers, E., Wallace, D.J. *Total synthesis of (–)-hemiasterlin, a structurally novel peptide that exhibits potent cytotoxic activity*. Tetrahedron Lett 1997, 38: 317-20.

19. Nunes, M., Kaplan, J., Loganzo, F., Zask, A., Ayral-Kaloustian, S., Greenberger, L.M. *Two photoaffinity analogs of HTI-286, a synthetic analog of hemiasterlin, interact with α-tubulin.* Eur J Cancer 2002, 38(Suppl. 7): Abst 396.

20. Lo, M.-C., Aulabaugh, A., Krishnamurthy, G., Kaplan, J., Zask, A., Smith, R.P., Ellestad, G. *Probing the interaction of HTI-286 with tubulin using a stilbene analog.* J Am Chem Soc 2004, 126: 9898-9.

21. Krishnamurthy, G., Cheng, W., Lo, M.-C., Aulabaugh, A., Razinkov, V., Ding, W., Loganzo, F., Zask, A., Ellestad, G. *Biophysical characterization of the interactions of HTI-286 with tubulin heterodimer and microtubules.* Biochemistry 2003, 42: 13484-95.

22. Loganzo, F., Hari, M., Annable, T. et al. *Cells resistant to HTI-286 do not overexpress P-glycoprotein but have reduced drug accumulation and a point mutation in α-tubulin.* Mol Cancer Ther 2004, 3: 1319-27.

23. Poruchynsky, M.S., Kim, J.-H., Nogales, E., Annable, T., Loganzo, F., Greenberger, L.M., Sackett, D.L., Fojo, T. *Tumor cells resistant to a microtubule-depolymerizing hemiasterlin analogue, HTI-286, have mutations in α- or β-tubulin and increased microtubule stability.* Biochemistry 2004, 43: 13944-54.

24. Wang, C.P., Talaat, R., Wang, J., Lin, M., Hultin, T., Scatina, J. *In vitro and in vivo metabolism of HTI-286, an antimicrotubule anticancer agent.* Drug Metab Rev 2003, 35(Suppl. 2): Abst 83.

25. Udata, C., Floss, D., Crawford, D., Tse, S., Leal, M., Hicks, D., Stroshane, R., Fluhler, E.N. *Species comparison and allometric scaling of HTI-286 (a novel hemiasterlin tubulin inhibitor) pharmacokinetics.* Annu Meet Am Assoc Pharm Sci (AAPS) (Nov 10-14, Toronto) 2002, Abst W5287.

26. Ratain, M.J., Undevia, S., Janisch, S., Roman, S., Mayer, P., Buckwalter, D., Foss, D., Hamilton, B.L., Fischer, J., Bukowski, R.M. *Phase 1 and pharmacological study of HTI-286, a novel antimicrotubule agent: Correlation of neutropenia with time above a threshold serum concentration.* Proc Am Soc Clin Oncol 2003, 22: Abst 516.